

# Experimental and Theoretical Study of Composite Cold Formed Steel-Concrete Beams

Nabil S. Mahmoud<sup>1</sup>, Saad El-Deen M. Abd-Rabou<sup>1</sup>, Mohamed Ghannam<sup>2</sup>, Ahmed A. Abdel-Kader<sup>3</sup>

<sup>1</sup>Prof. of steel structures, Mansoura University, Mansoura, Egypt

<sup>2</sup>lecturer in structural Engineering Department, Mansoura University, Mansoura, Egypt

<sup>3</sup>Assistant Lecturer in structural Engineering Department, Mansoura University, Mansoura, Egypt

**Abstract:** *This paper presents an experimental investigation and theoretical analysis using finite element model for composite cold formed steel beams. Experimental tests are carried on full scale composite cold formed steel (CFS) beams. The steel beams consist of two cold formed steel channel sections back to back which connected to a reinforced concrete slab using new means to transfer the shearing force between them to achieve the composite action. Two groups of beams have been tested. In the first group, the composite action has been achieved using the embedment of the upper part of steel section inside the concrete slab. In the second group, the composite action is achieved using the reforming of the steel flange inside the concrete slab to act as shear connectors. The parameters studied in the first group are the ultimate strength of the concrete, height of the embedded part of the steel section in the RC slab, effect of the interaction between shear and bending moment depending on the loading method, the direction of the applied load with respect to the beam position, and effect of encasing steel web with concrete. While the studied parameter in the second group, is the spacing between the new shear connectors developed from the reforming of the steel section flange. The beams' ultimate strengths, load-mid span vertical deflection relationships and failure modes of the beams have been recorded from the tests. The finite element analysis has been performed using ABAQUS. The ultimate strengths and failure modes from nonlinear analysis are compared with the experimental results to verify the accuracy of the developed models.*

**Keywords:** composite cold formed steel beams; finite element; experimental results; shear connector; composite action

## 1. Introduction

Cold-formed steel (CFS) sections, usually with thickness between 1.2 mm to 6 mm, have been recognized as an important contributor to sustainable structures in the developed nations. Recent studies on composite beams with CFS were reported by other researchers who agree about their application in modern constructions. However, there remains a lack of data on the behavior and performance of CFS in composite construction. One limiting disadvantage of CFS is the thickness of its section that makes it susceptible to local, distortional, lateral torsional buckling. Hence, using a composite construction of reinforced concrete deck slab and structural CFS section is a practical solution. This reduces the distance from the neutral-axis to the top of the deck slab. As a result, this would reduce the compressive bending stresses in the CFS sections and ameliorate buckling problem. Composite beams made of concrete with cold-formed steel channels as soffits and embossment as connectors were tested by George and Richard [1, 2]. Deric, et al. studied reinforced concrete beams with cold-formed steel sheets bending in the soffit and Sides of the beams wherein the trapezoidal profiles in the steel sheet acted as connectors [3]. Ahmed F. El-min tested fifteen composite beams having six steel plate shapes with thickness of 10 mm. Steel connectors were formed using nails fixed through drilled holes in steel plate by means of epoxy [4]. L. M. Abdel Hafez performed nonlinear studies on composite CFS beams using ANSYS program to simulate the behavior of cold-formed bi-steel-concrete beams conducted by Ahmed F. El-min and to cover various parameters that were not taken into account experimentally such as nail diameter and concrete strength effect [5]. Experiments on Sixteen specimens consisting of three series B, C and R representing respectively box, channel and reinforced concrete beams of effective span 1440 mm were considered in the investigation by T. ValsaIpe and H. Sharada Bai to study the effect of the shape of the steel section and the position of the shear connectors and to compare

the cold formed composite sections with the RCC beams [6]. Wissam D. Salman (2014) carried out experimental tests on seven composite steel-concrete tube beams taking into account the effect of diameter and thickness of steel tube on structural performance of composite beams [7]. Experimental results proved that increasing tube thickness or diameter would enlarge the strength and the ultimate deflection increased and a FE element model was used to verify the obtained results using ANSYS. In this study, the behavior of composite cold formed steel beams with cold formed steel section were investigated experimentally and numerically using nonlinear 3-D finite element model by ABAQUS [8]. Two groups of full-scale CFS composite beams were loaded up to failure as shown in fig (1). The first one is composed of seven CFS composite beams, the shear interaction between the concrete and the steel beams of group (A) is achieved using the embedment of the upper steel flange inside the concrete slab as shown in fig (1.a). These beams are loaded using two methods of loading; the first method is carried under three point bending test at mid span, so the beam section is exposed to a combination between shear force and bending moment, the second method is done using four point bending test with one meter space between the intermediate applied loads, so the beam section is exposed to a pure bending moment on the portion between the two intermediate loads. To study the negative bending moment effect, the tested beam is inverted, so the steel section is in the compression side and concrete slab is located in the tension side. The embedded heights of the steel section that have been used are 20 and 50 mm. Concrete strengths of the normal concrete strength ( $f_{cu}$ ) are 23, 41 and 59 MPa. Partially encased composite beams with thin thickness are used to study local buckling effect. The second group (B) is composed of two CFS composite beams. The shear interaction is achieved by reforming the upper flange of steel section to act as a shear connector between the steel and the concrete as shown in fig (1. b). These beams are loaded by one concentrated load.

2. Experimental work

This section highlights the test program undertaken. The test set-up for the tested CFS composite beams is described. Experimental results and failure modes have been recorded.

2.1 Test specimens

The test program contains two groups of beams; the first group (A) is composed of seven specimens (A-1, A-2, A-3, A-4, A-5, A-6, A-7) and the second is group (B) consists of two specimens (B-1, B-2). Also, the all tested beams have the same steel cross section of two cold formed channels back to back connected together with screw bolts (4.0mm diameter and 40mm length) as shown in the fig (1). The steel section is connected with reinforced concrete (RC) slab of dimensions shown in fig (1). The concrete slab is reinforced by four longitudinal bars of 10 mm diameter and lateral bars 10 mm diameter spaced by 200 mm. For the tested beams of group

(A), the upper part of the steel section has been embedded inside the concrete slab with a certain height as shown in fig (1-a). While the steel sections of group (B) are connected to the concrete slab by means of a new suggested shear connector obtained from the reforming of the steel flange of the steel section with spaces (s) as shown in fig (1-b). Push out tests have been tested previously to determine the capacity of the used shear connector [9]. The studied parameters in the tests of group (A) are the ultimate strength of the concrete cube after 28 days ( $f_{cu}$ ), the height of the embedded part of the steel section in the RC slab (hemb.), effect of the interaction between shear and bending moment depending on the loading method, the direction of the applied load with respect to the beam position, and effect of encasing steel web with concrete. While the distance between the shear connectors along the beam is the studied parameter in group (B). These parameters of the specimens are illustrated in table (1).

Table 1: The tested beams properties and the studied parameters

Specimens	Studied Parameters				
	$h_{emb}$ (mm)	Web encasement	Loading Method	S (mm)	$f_{cu}$ (Mpa)
A-1	20	50cm at the both ends	1-point load (mid-span)	----	23
A-2	50	50cm at the both ends	1-point load (mid-span)	----	59
A-3	50	50cm at the both ends	2-point loads spaced 1m	----	59
A-4	20	50cm at the both ends	1-point load (mid-span)	----	59
A-5	20	The whole length	1-point load (mid-span) (negative)	----	59
A-6	50	The whole length	1-point load (mid-span)	----	59
A-7	20	50cm at the both ends	1-point load (mid-span)	----	41
B-1	----	The whole length	1-point load (mid-span)	15	41
B-2	----	The whole length	1-point load (mid-span)	30	41

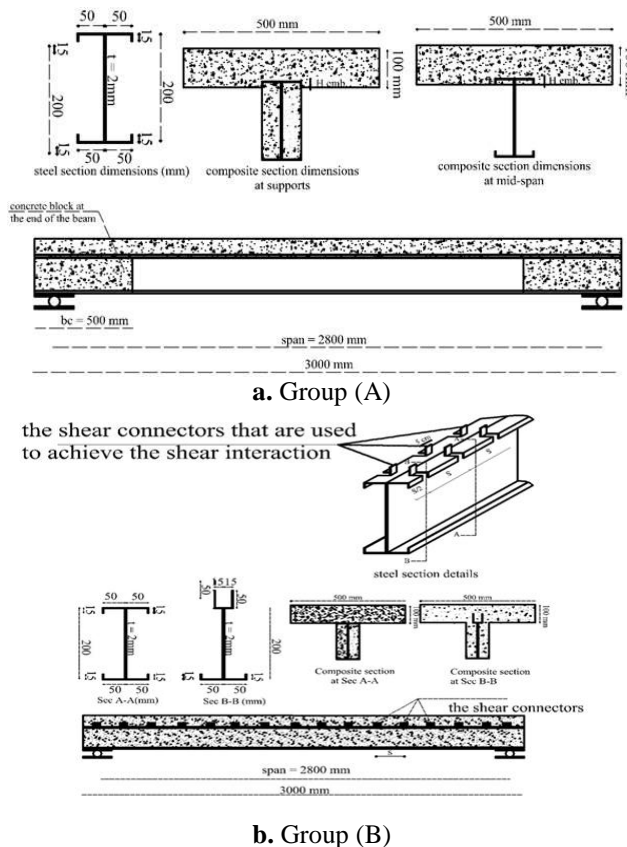


Figure 1: The details of the beams specimens and the cross sections of group (A) and group (B)

2.2 Material Properties

2.2.1 Reinforced steel

Three steel tensile coupon tests were carried out to determine the stress-strain curve of the steel plate. Properties including the yield stress ( $f_y$ ), ultimate tensile stress ( $f_u$ ) and Young’s modulus of elasticity ( $E_s$ ) of the steel sections and longitudinal reinforcing bars used are listed in table (2).

Table 2: Mechanical properties of the used steel and the reinforcing steel

Type	$f_y$ (t/cm <sup>2</sup> )	$f_u$ (t/cm <sup>2</sup> )	$E_s$ (t/cm <sup>2</sup> )
Steel section	2.35	2.90	2060
Reinforcing bar	3.60	4.60	2010

2.2.2 Concrete

The used concrete mixes used are designed to achieve a compressive capacity 23 MPa, 41 MPa and 59 MPa as shown in table (3).

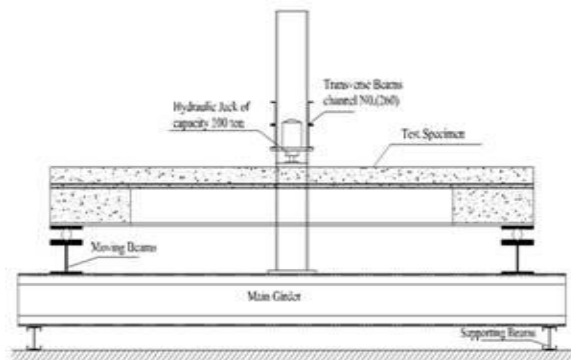
Table 3: Concrete mixes used in the experiments

The component	$f_{cu}=23$ MPa	$f_{cu}=41$ MPa	$f_{cu}=59$ MPa
Cement	300 kg	500 kg	500 kg
Gravel	1200 kg	1074 kg	1142 kg
Sand	800 kg	576 kg	620 kg
Water	150 kg	215 kg	150 kg
Super plasticizers	-----	-----	20 kg

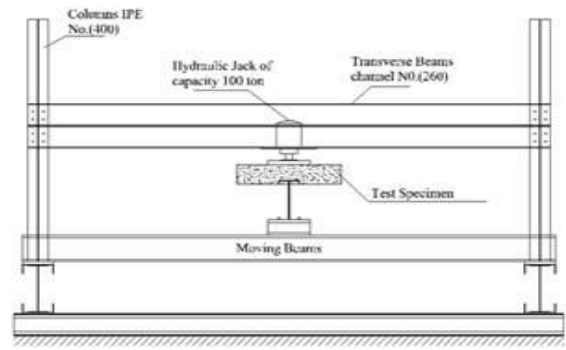
2.2.3 Test Set-up

The composite beams were rested on rollers on both sides and were exposed to one concentrated load at mid-span or two equal point loads spaced by one meter. The applied loads in all tests were carried out using calibrated hydraulic jack connected with an electric hydraulic pump with capacity of 100 ton as shown in Fig (2).

For each test, the mid-span vertical deflection has been recorded using dial gauges of 0.01mm accuracy. During the testing operation, the tested load is applied on the specimen in a constant incremental rate of 0.5 ton each 10 minutes. During the loading, the outer beam surface was carefully investigated and the propagation of cracks was followed and marked. All sides of the test were secured before starting of loading the beam.



a. side view of the main testing frame



b. elevation of the main testing frame

Figure 2: Test setup

3. Experimental Results

The experimental results include the recorded failure loads ( $P_{test}$ ), the mid span vertical deflection ( $\delta_{test}$ ) and their associated failure modes for each tested beam.

3.1 Recorded Mid-Span Vertical Deflection

The relationship between the applied load and the recorded the mid-span vertical deflection for all tested beams is shown in Figure (3.a) and Figure (3.b). Table (4) illustrates the section bending capacity ( $M_{test}$ ) from test results which is related to the ( $P_{test}$ ) and the mid span vertical deflection corresponds to the ultimate load ( $\delta_{Exp}$ ) as shown in the Figure (3.a). To study the effect of the parameters on the deflection, the load should be taken as a constant. The deflection has been taken which corresponds to ( $P=5.0$  ton). For group (A), it is noticed from the results of beams (A-2) & (A-4) that the deflection of the beam corresponds to the ( $P=5.0$  ton) increases 80.8 % when increasing the embedded height from 2cm to 5 cm. Also, it is found from the results of beams (A-1), (A-4) & (A-7) that the deflection of beam corresponds to ( $p=5$ ton) decreases 45.967 % when increasing the  $f_{cu}$  from 23 MPa to 59 MPa and decreases by 27.533 % when increasing  $f_{cu}$  from 23 MPa to 41 MPa. Also, it is noticed from the results of beams (A-2) & (A-6) that the deflection corresponds to ( $p=5$  ton) decreases by 64.44 % when using concrete encasement around the steel web. For group (B), it is noticed that the deflection corresponds to ( $P=5$  ton) increases by 30.7 % because of the increasing of the spacing (S) from 15 cm to 30 cm.

3.2 Ultimate Strength of The Tested Beams

From table (4), it is noticed that the beam strength of beams (A-1) increases 11.3% due to increasing  $F_{cu}$  from 23 MPa to 59 MPa and increases 6.832% due to increasing  $F_{cu}$  from 23 MPa to 41 MPa. It is noticed that the beam strength of beam (A-2) increases 6.67 % due to decreasing embedded height ( $h_{emb}$ ) from 5 cm to 2cm because of the increasing of the inertia of the beam section. Also, it is noticed that the beam strength of beam (A-2) increases 25% when subjected to pure bending moment only without shearing force. It is found that the beam strength increases from beam (A-2) increases by 8.33% due to the encasement of the steel web of the beam with plain concrete, Also, from Figure (3.a), it is observed that the beam strength of (A-4) decreases 51.56% when the

beam section is subjected to negative moment as appeared from the behavior of beam (A-5).

It is also observed that the effect of the spacing between the shear connectors between 15cm and 30 cm have slight effects on the results of the beam capacity of group (B) which indicates almost a full composite action between steel and concrete either spaces (s) of 15 or 30 cm. The failure mode shape and stress distribution are shown in Figure (6) and Figure (11). Also, from the first principles of the structure, it is found that the shear interaction per one cm on the suggested shear connector on beams (B-1), (B-2) equal 0.234 t/cm so the shearing force acts per one shear connector on beam (B-1) equal 3.514 ton and for beam (B-2) equal 7.012 ton. Figure (4) shows the relation between the ( $P_{test}$ ) and ( $M_{test}$ ) for all the tested beams.

### 3.3 Toughness Modulus

Table (4) shows the toughness modulus for all the tested beams. The toughness modulus is equal to the area under the P- $\delta$  curve which represents the amount of the work done during the loading of the beam. It is noticed from the results of beams (A-2) and (A-4) that the toughness modulus of the beam increases 36.08% with the decreasing of the embedded height from 5 cm to 2 cm. It is noticed from the results of beams (A-1), (A-4) and (A-7) that the toughness modulus increases 73.08% by increasing  $f_{cu}$  from 23 MPa to 59 MPa and increases 41.56% by the increasing of  $f_{cu}$  from 23 MPa to 41 MPa. Also, it is found from the results of (A-2) and (A-6) that the toughness increases slightly with the encasement of the steel web with concrete. From the results of group (B), it is noticed that the toughness modulus decreases 25.05% by the increasing of the spacing (S) from 15 cm to 30 cm.

### 3.4 Composite Action Degree ( $\xi$ )

From table (4), it is noticed that the Composite Action Degree of beam (A-1) increases 3.14 % due to increasing  $F_{cu}$  from 23 MPa to 59 MPa and increases 0.104 % due to increasing  $F_{cu}$  from 23 MPa to 41 MPa. It is noticed that the Composite Action Degree of beam (A-2) decreases 14.57 % due to decreasing embedded height ( $h_{emb}$ ) from 5 cm to 2cm because of the increasing of the inertia of the beam section. Also, it is noticed that the composite action degree of beam (A-2) increases 65.13 % when subjected to pure bending moment only without shearing force. It is found that the composite action degree increases from beam (A-2) increases by 21.7% due to the encasement of the steel web of the beam with plain concrete. Also, from Figure (4.12), it is observed that the composite action degree of (A-4) decreases 61.63% when the beam section is subjected to negative moment as appeared from the behavior of beam (A-5).

It is also observed that the effect of the spacing between the shear connectors between 15cm and 30 cm have slight effects on the results of the beam capacity of group (B) which indicates almost a full composite action between steel and concrete either spaces (s) of 15 or 30 cm.

## 4. Finite Element Modeling

### 4.1 Finite Element Types

The composite beam components were modeled using a combination of 3-D solid element (C3D8) for concrete, longitudinal bars, and steel section, available in ABAQUS/CAE element library, as shown in Figure 8. The partition of the elements is made to be suitable for the other elements. Different mesh sizes were tried to choose a suitable mesh that provide both reliable results and less computational time, a mesh 50mm depth can achieve accurate results with average aspect ratio equal 2.1.

### 4.2 Boundary Conditions

To give reliable simulation of the beams on the finite element (FE), one end of the beams was presented in the finite element modeling as a hinge rotating about the bending axis, and the other end of the beams was presented as roller allowing displacement in the direction of the axis of the beam and rotation about the bending axis. A concentrated load is applied and connected with a part of slab upper surface with length of concrete slab and width of 100 mm to simulate the steel plate used in loading procedures. The connection is achieved using COUPLING option available in the ABAQUS/CAE. The analysis method used is static general analysis including the nonlinear geometric effect.

### 4.3 Material Properties

Since no tests were made to estimate Young modulus and Poisson ratio, concrete Young modulus  $E_c$  is calculated as recommended by the Euro code part 2 [10, 11] and Poisson ratio is 0.2. Concrete Damage Plasticity model is used to simulate the concrete behavior in which, dilation angle, biaxial stress ratio and the tensile-to-compressive meridian ratio were assumed to be equal to 30, 1.16, and 0.667 respectively. The tensile strength of the concrete is considered to be 10% of the compressive strength with tensile softening response characterized by means of fracture energy (GF)

$$G_F = (0.0469d_{max}^2 - 0.5d_{max} + 26) (f_c' / 10)^{0.7} \text{ N/m} [12, 13]$$

Where  $f_c'$  is in Mpa,  $d_{max}$  is the maximum coarse aggregate size (in mm), if  $d_{max}$  had not been reported in a reference, it was taken as 20 mm. While the Young modulus of steel and longitudinal bars is shown in table (3) and Poisson ratio  $\nu = 0.3$ .

### 4.4 Interaction between Steel and concrete

The interaction between the steel and concrete was defined as contact with a tangential behavior (friction formulation: penalty) with coefficient of friction = 0.6, but to determine the suitable coefficient of friction suitable for the model we made a sensitivity analysis, and normal behavior (pressure over-closure: hard contact). The nails connecting two steel sections are modeled using springs with linear elastic stiffness of 0.1 ton/mm to simulate the axial behavior of the nails.

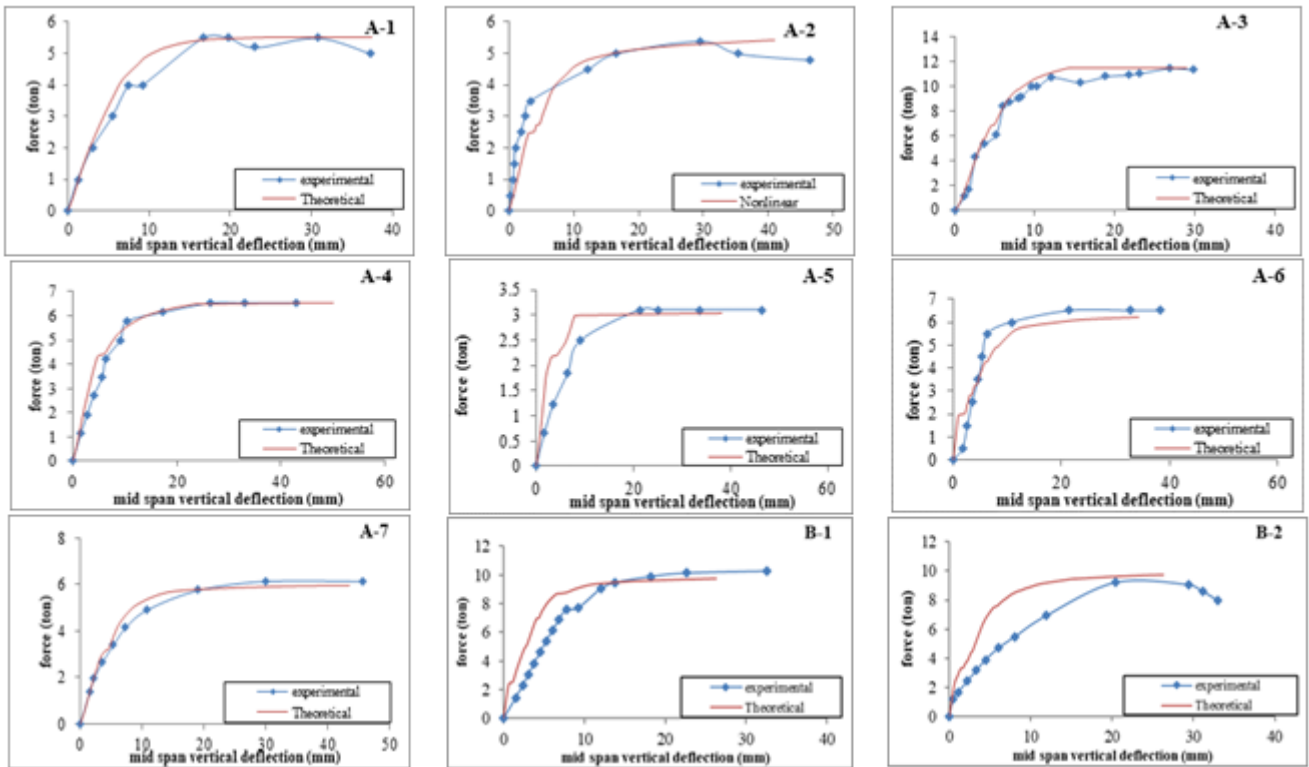


Figure 3: Comparison between experimental and non-linear analysis results for the tested beams

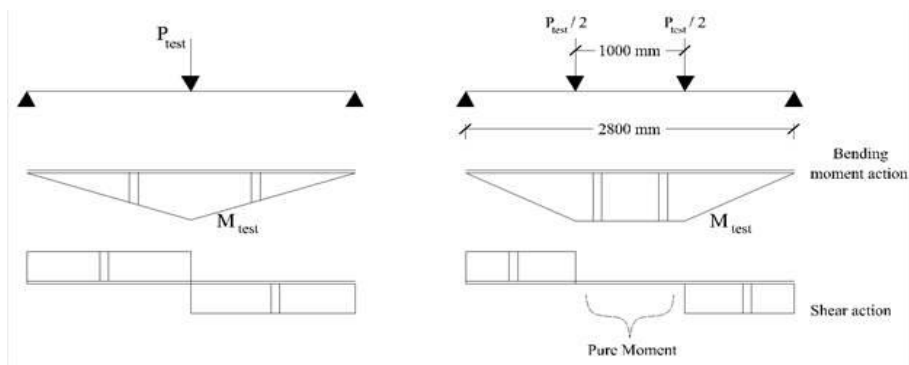


Figure 4: The section bending capacity ( $M_{test}$ ) from test results which is related to the ( $P_{test}$ )



Figure 5.a: Longitudinal cracks in the concrete slab beam followed by flexural buckling of the upper flange and web of steel section in the mid span (A-2)



**Figure 5.b:** Cracks appeared in the surface of the concrete slab (A-4)



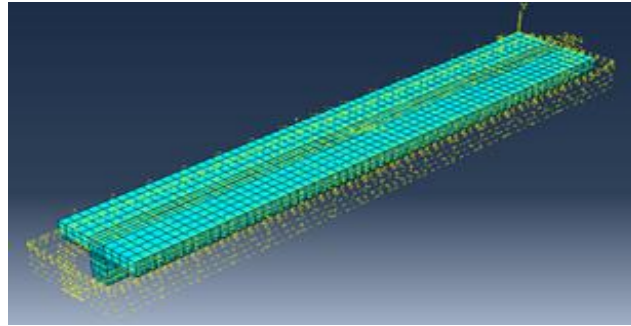
**Figure 5.c:** Web encasement effect (A-6)



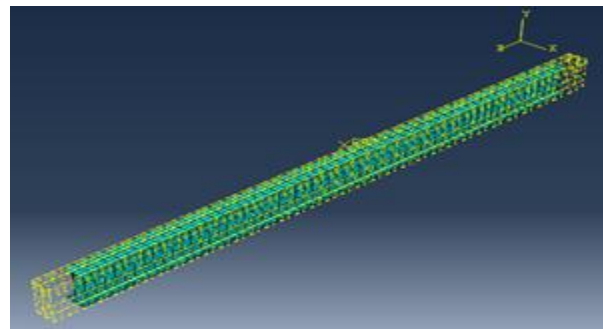
**Figure 5.d:** Cracks in the concrete slab followed by plastic hinge appeared in the mid span (A-5)



**Figure 6:** Concrete cracks in the mid span (B-2)

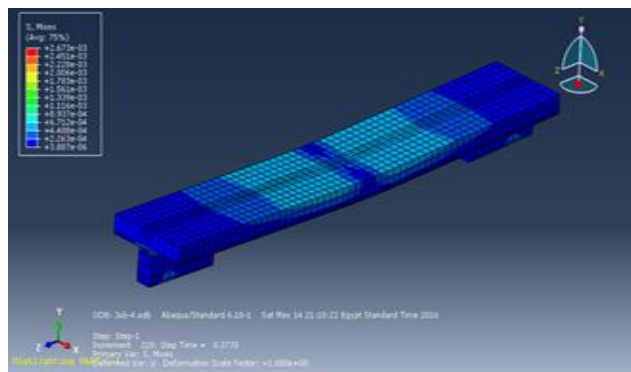


a: Concrete slab

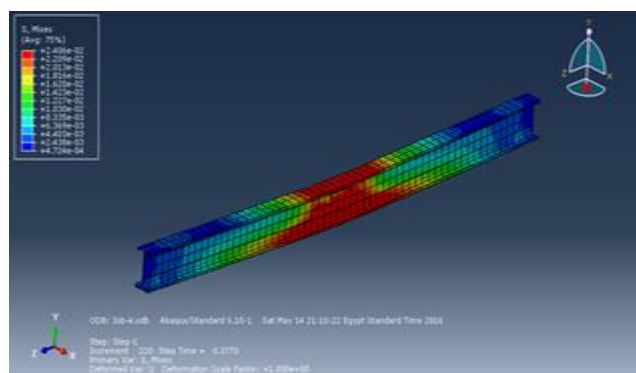


b: Steel section

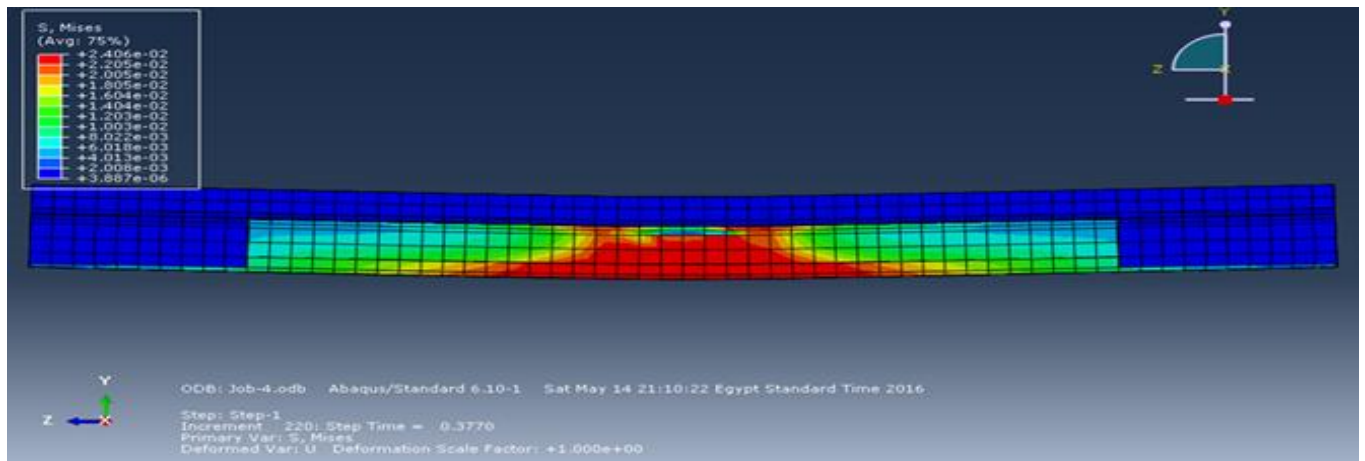
Figure 7: Meshing details of the beam components using ABAQUS



a: Stress distribution on the concrete slab only



b: Stress distribution on the steel section only



c: Stress distribution on the whole section

Figure 8: The stress distribution on the composite beam obtained from the finite element

Table 4: Experimental and theoretical results for all tested beams

Spec. No.	Studied Parameters					Results						
	h <sub>emb</sub> (mm)	Web Encasement	Loading Method	S mm	f <sub>cu</sub> MPa	M <sub>0%</sub> cm.t	M <sub>100%</sub> cm.t	P <sub>FE</sub> ton	M <sub>FE</sub> t.cm	δ <sub>FE</sub> mm	T <sub>FE</sub> t.mm	ξ <sub>FE</sub> (%)
								P <sub>exp.</sub> ton	M <sub>exp.</sub> t.cm	δ <sub>exp.</sub> mm	T <sub>exp.</sub> t.mm	ξ <sub>exp.</sub> (%)
A-1	20	50cm at the both ends	1-point load (mid-span)	----	23	253.7	563.9	5.52	386.9	17.81	180.6	42.9
								5.75	402.5	18.81	169.3	47.96
A-2	50	50cm at the both ends	1-point load (mid-span)	----	59	258.8	543.2	5.8	406	29.05	188.8	51.75
								6	420	30.32	215.3	56.68
A-3	50	50cm at the both ends	2-point loads spaced 1m	----	59	258.8	543.2	11.4	515.8	13.95	281.6	90.36
								11.6	525	12.12	275.8	93.6
A-4	20	50cm at the both ends	1-point load (mid-span)	----	59	258.8	641.2	6.2	434	24.64	293	45.81
								6.4	448	26.56	293.7	49.47
A-5	20	The whole length	1-point load (mid-span) (negative)	----	59	160.3	458.9	3.04	213.1	16.54	107.4	17.68
								3.1	217	21.31	124.7	18.98
A-6	50	The whole length	1-point load (mid-span)	----	59	258.8	543.2	6.15	430.5	28.03	198.3	60.37
								6.5	455	27.98	216.2	68.98
A-7	20	50cm at the both ends	1-point load (mid-span)	----	41	257.2	617.1	5.98	418.7	24.51	229.3	44.87
								6.14	430	22.81	239.7	48.01
B-1	----	The whole length	1-point load (mid-span)	15	41	257.2	682.4	9.75	682.7	26.24	222.2	100.1
								10.2	719	20.29	270	108.6
B-2	----	The whole length	1-point load (mid-span)	30	41	257.2	682.4	9.73	681.6	26.25	216.6	99.81
								9.62	674	21.41	202.4	98.02

Where:

$\xi$  (%) =  $[M - M_{0\%}] / [M_{100\%} - M_{0\%}]$ ,  $M_{100\%}$  is the moment capacity of the beam section in the case of full composite action,

$M_{0\%}$  is the moment capacity of the beam section in the case of no composite action.

## 5. Comparison between Experimental and Theoretical Results

### 5.1 Ultimate Load

Table (6) shows comparison between the nonlinear analysis results and the experimental results of the ultimate load for each beam of the tested beam. The comparison indicates that

for the beams of group (A) (A-1), (A-2), (A-3), (A-4), (A-5), (A-6) and (A-7), the difference between the nonlinear results and the experimental results is 4.827%, 5.45%, 2.313%, 0.459%, 1.935%, 5.384% and 2.605% respectively.

For beams of group (B), the difference between the analytical failure load and the experimental failure load for beams (B-1) and (B-2) are 5.06% and 1.14%. Comparison between the test results and the calculated results from the finite element ABAQUS are presented in table (5.1) and Fig (9). From table (6), it is noticed that a good agreement with a mean value of 1.026 and a coefficient of variance of 0.02473 for the strength ratio ( $P_{test}/P_{FE}$ ). Fig (9) shows a comparison between the finite element and the experimental ultimate load for the tested beams.

**Table 6:** Comparison between the Experimental values of the failure load and that calculated from nonlinear analysis

Tested beam	Ultimate load (ton)		Exp./nonlinear
	experimental	Nonlinear	
A-1	5.75	5.52	1.04
A-2	6	5.8	1.05
A-3	11.6	11.4	1.0186
A-4	6.4	6.2	1.01
A-5	3.1	3.04	1.018
A-6	6.5	6.15	1.056
A-7	6.14	5.98	1.028
B-1	10.2	9.75	1.05
B-2	9.62	9.73	0.98
Mean			1.026
Coefficient of variation			0.02473

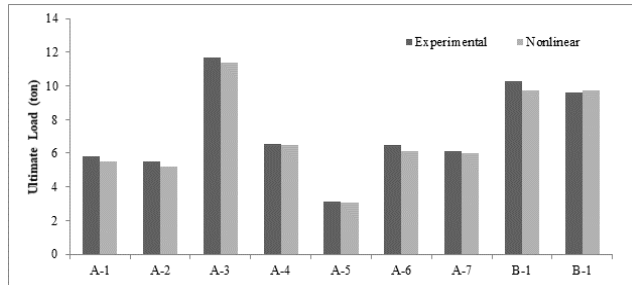


**Figure 9:** Comparison between the finite element and the experimental ultimate load for the tested beams

**5.2 Mid span Vertical Deflection**

Table (7) shows comparison between the nonlinear analysis results and the experimental results of the maximum vertical deflection in the mid span for each beam of the tested beams. The comparison indicates that for the beams of group (A) (A-1), (A-2), (A-3), (A-4), (A-5), (A-6) and (A-7), the difference between the nonlinear results and the experimental results is 5.316 %, 4.188%, 15.09%, 7.228%, 22.383%, 0.1786% and 7.45 % respectively.

For beams of group (B), the difference between the analytical maximum mid span deflection and the experimental

maximum deflection for beams (B-1) and (B-2) are 29.32% and 22.6%. Comparison between the test results and the calculated results from the finite element ABAQUS are presented in table (7) and Fig (10). From table (7), it is noticed that the mean value of 1.036 and a coefficient of variance of 0.214 for the deflection ratio ( $\delta_{test}/\delta_{FE}$ ) which means that there is a quite difference in the values of the deflection between the finite element modeling and the experimental work. Fig (10) shows a comparison between the finite element and the experimental mid-span vertical deflection for the tested beams.

**Table 7:** Comparison between the Experimental values of the mid span vertical deflection and that calculated from nonlinear analysis

Tested beam	Maximum mid span deflection (mm)		Exp./nonlinear
	experimental	nonlinear	
A-1	18.81	17.81	1.05
A-2	30.32	29.05	1.04
A-3	12.12	13.95	0.86
A-4	26.56	24.64	1.07
A-5	21.31	16.54	1.28
A-6	27.98	28.03	0.99
A-7	22.81	24.51	1.46
B-1	20.29	26.24	0.77
B-2	21.41	26.25	0.81
Mean			1.036
Coefficient of variation			0.214

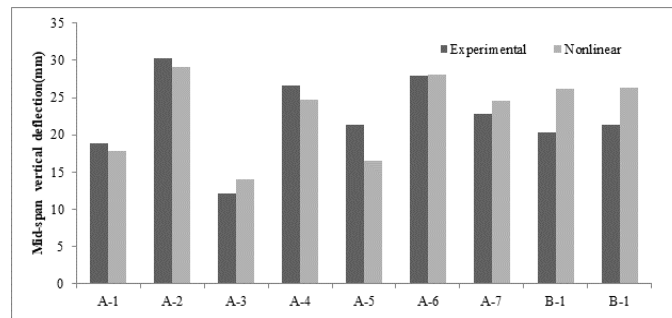


Figure 10: Comparison between the finite element and the experimental mid-span deflection for the tested beams

## 6. Conclusion

From the results and discussions presented in this work, the following conclusions can be drawn:

- A comparison between the numerical and experimental results for composite cold formed steel beams using the new suggested means of shear connection shows a good agreement. The mean value and coefficient of variation of test strength to non-linear strength ratio ( $M_{test}/M_{FE}$ ) is 1.026 and 0.02473, respectively. Also, the mean value and coefficient of variation of test deflection to non-linear deflection ratio ( $\delta_{test}/\delta_{FE}$ ) is 1.036 and 0.214 respectively. This means that FE method give a good agreement with test results.
- From the results of the beams of group (A):
  - a. It is noticed that the deflection increases with the increasing of the embedded height inside the concrete slab and decreases with the concrete encasement around the steel web and with increasing of  $f_{cu}$  of the concrete.
  - b. It is found that the ultimate moment capacity increases with the decreasing of the embedded height inside the concrete slab because of the increasing of the inertia of the section
  - c. It is found that the ultimate moment capacity with the concrete encasement around the steel web and with the increasing of  $f_{cu}$ .
  - d. It is noticed that the deflection increases with the increasing of the embedded height inside the concrete slab and with increasing of  $f_{cu}$  of the concrete and decreases with the concrete encasement around the steel web.
  - e. It is found that the ultimate moment capacity increases with the decreasing of the embedded height inside the concrete slab and with the concrete encasement around the steel web and with the increasing of  $f_{cu}$  and when the section is subjected to pure moment.
- From the results of the beams of group (B):
  - a. It is found that the deflection increases with the increasing of the spacing (S) between the suggested shear connectors.
  - b. It is noticed that the ultimate moment doesn't effected by the increasing of the spacing (S) between the shear connectors.
- From the results of the beams of group (A) and (B), the type of the shear connector used in beams of group (B) is better than used in beams of group (A)

## References

- [1] George Abdel-Sayed. (1982) "Composite Cold-Formed Steel-Concrete Beams", Journal of the Structural Division, ASCE, Vol. 108, No. ST11, 2609-2622.
- [2] Richard P. Nguyen. (1991) "Thin-Walled Cold-Formed Steel Composite Beams", Journal of Structural Engineering, ASCE, 117 (10), pp. 2936-2952.
- [3] Deric J. Oehlers; Howard D. Wright; Matthew J. Burnet (1994) "Flexural Strength of Profiled Beams", Journal of Structural Engineering, ASCE, 120 (2), pp. 378-393.
- [4] Ahmed Fathalla Mohamed El-min, "Structural Behavior of Bi-Cold Deformed Steel Concrete Composite Beams", Civil Eng. Dept., Faculty of Eng., Assuit University, Assuit, Egypt, 2005
- [5] L. M. Abdel Hafez, "Analysis of Bi-cold formed steel concrete composite beams", Civil Eng. Dept., Faculty of Eng., Minia University, Minia, Egypt, 2006
- [6] T. ValsaIpe; H. Sharada Bai (2015) "An Experimental Study On The Positioning Of Shear Connectors In Steel-Concrete Composite Beams", the 2015 world congress on advances in structural engineering and mechanics (ASEM15), Incheon, Korea
- [7] Wissam D. Salman (2014)"strength and behavior of composite steel tube concrete beam", diyala journal of engineering science, vol.8, no.2, pp163-181
- [8] ABAQUS. ABAQUS standard user's manual, version 6.10. Dassault Systèmes Corp.: Providence, RI (USA); 2010
- [9] Nabil S. Mahmoud, Saad El-deen M. Abd-rabou, Mohamed ghannam and Ahmed A. Abdel-kader." Proposed Formula for Shear Resistance of Innovative Shear Connector between Cold Formed Steel Section and Concrete." Mansoura Engineering Journal, (MEJ), VOL. 43, ISSUE 1, March 2018
- [10] Euro code 2, Design of Concrete Structures, Part 1-1: General Rules and Rules for Buildings, 2004.
- [11] CEN (2005d). EN 1993-1-10:2005 – Euro code 3: Design of Steel Structures, Part 1.10: Material toughness and through thickness properties, European Committee for Standardization, Brussels.
- [12] FIP. CEB-FIP Model Code 1990. London: Thomas Telford Ltd.; 1993.
- [13] Bažant ZP, Becq-Giraudon E. Statistical prediction of fracture parameters of concrete and implications for choice of testing standard. Cement Concrete Res 2002;32 (4):529–56